



ELSEVIER

Journal of Molecular Structure (Theochem) 419 (1997) 85–95

THEO
CHEM

A note on the application of the “Boltzmann simplex”-simulated annealing algorithm to global optimizations of argon and water clusters

Francis M. Torres, Eugene Agichtein, Leonid Grinberg, Guowei Yu, Robert Q. Topper*

Department of Chemistry, The Cooper Union for the Advancement of Science and Art, Albert Nerken School of Engineering, 51 Astor Place, New York, NY 10003, USA

Received 1 November 1996; accepted 5 February 1997

Abstract

We report our application of a recently published simulated annealing algorithm which we call “Boltzmann simplex”-simulated annealing (BSSA) to global optimizations of argon and water clusters. The Lennard–Jones model of argon clusters serves as a challenging benchmark for global optimization methods, and we use it as a test case. We find that the BSSA method is most useful when followed by a local optimization via the Powell method. This is because the Powell method quenches to the equilibrium geometry more effectively than a downhill simplex, which is the zero-temperature limit of the BSSA algorithm. We also find that very slow annealing rates are required to achieve acceptable results. A study of small water clusters $[(\text{H}_2\text{O})_m]$, $m = 2\text{--}6$ using a recently published flexible-monomer interaction potential yields ring-like structures which are in good agreement with other theoretical and experimental studies for $m = 3\text{--}5$. A highly puckered ring structure is obtained for $m = 6$. © 1997 Elsevier Science B.V.

Keywords: Water clusters; Simulated annealing; Optimization methods

1. Introduction

The study of atomic and molecular clusters is yielding a wealth of information about interatomic and intermolecular forces [1]. As we learn more about these forces we can, in principle, use what we learn to improve our understanding of bulk phases of materials through computational simulations of their dynamical and thermal properties [2,3].

For this reason, clusters have been the subject of many recent theoretical and experimental studies [1–3]. Such studies ultimately should shed light on which intermolecular potential models are reliable

for computer simulations of the bulk materials. From our perspective, an interesting question can be posed in the light of what we know so far about water in its bulk and cluster phases: if a potential or theoretical method works well for liquid water, will it work well for water clusters? And what about in the reverse direction? Will well-tuned cluster potentials yield accurate results for liquid water? Moreover, to what extent are these conclusions true for other substances, such as metals, inorganic salts and organic compounds?

In order to answer the preceding questions one must have an energetic model for the cluster of interest. Once this is obtained, one must next somehow survey the potential energy surface of the cluster. One class

* Corresponding author.

of techniques available for this latter purpose are simulated annealing algorithms. These algorithms are basically the coupling of a temperature-controlled geometry fluctuation scheme, such as Monte Carlo, Brownian dynamics or molecular dynamics [4], to a scheduled temperature variation which slowly quenches the cluster down to an energy minimum. If quenching is rapid, local minima are generally located; if infinitely slow, the global minimum can be obtained (assuming that the highest temperature of the annealing schedule is high enough). These fluctuation schemes all have varying degrees of algorithmic complexity, numerical efficiency and ease of implementation. For example, molecular dynamics and Brownian dynamics both require the programmer to implement energy derivatives, usually explicitly, to obtain interatomic forces; Monte Carlo does not [3,4]. However, successful Monte Carlo work relies on the development of efficient and ergodic sampling strategies whereas in molecular and Brownian dynamics, all sampling is generated by the solution of the differential equations to be solved [4]. The numerical solution of these differential equations also poses certain numerical challenges that must be dealt with [4]. In addition, most fluctuation algorithms rely to some extent on the availability of high-quality random number generators with reasonably long recurrence times [4,5]. There are no simple guidelines for deciding which of the many available alternatives is most appropriate for a given application. Therefore, experimentation with new methods is of some interest.

A new fluctuation scheme, which we have coined the ‘‘Boltzmann simplex,’’ was recently proposed by Press et al. in the second edition of their well-received text *Numerical Recipes* [5]. This new algorithm caught our attention as we began our studies of cluster systems. Their algorithm, which is essentially a downhill simplex algorithm with thermally-smearred vertex energies, does not require one to code the derivatives of the potential energy function, which makes debugging new cluster systems relatively easy and makes it possible to study systems easily when analytical energy derivatives may not be available. In addition, the algorithm reduces to a simplex algorithm in the limit of zero temperature, which has well-known convergence properties in the vicinity of a local minimum. However, Press et al. presented their algorithm without testing it in the context of computational

molecular modeling. These facts, combined with our interest in clusters, led us to investigate the algorithm’s properties extensively by testing it on three distinct types of cluster system.

When testing new algorithms, benchmarks are essential. We began by considering argon clusters within a pairwise-additive Lennard–Jones potential. Hoare and Pal [6,7] have presented minimum-energy structures and vibrational frequencies for small Lennard–Jones clusters, and we use their results as a benchmark to test the efficacy of the BSSA algorithm and to assess the appropriate selection of annealing parameters.

We also consider small water clusters within an interaction potential recently proposed by Ferguson [8]. The Ferguson potential, a flexible-water model which is a modification of the well-known SPC rigid model [9], was shown by NPT molecular dynamics simulations to reproduce a number of the experimental properties of liquid water at 298 K and 1 atm. These properties include the radial distribution functions, the dielectric constant, the vibrational spectrum, the self-diffusion constant, and the free energies of solvation for neon atoms and water molecules [8]. We have obtained minimum-energy structures within this model for water clusters with up to six monomers, and we here compare the results with recently obtained experimental values [10] as well as published ab initio, density-functional theory and model potential results. Ultimately we hope to begin to address the question of whether a potential which is well-parameterized for reproduction of the bulk’s properties can predict the properties of clusters. Furthermore, the results of the present study could be used to achieve further fine-tuning of the potential if necessary.

2. Computational methods

To explore the potential energy surfaces of the clusters we have considered, we have implemented an algorithm recently presented by Press et al. [5] which they refer to as ‘‘continuous minimization by simulated annealing’’. The word ‘‘continuous’’ refers to the continuous nature of the function to be optimized, emphasizing the fact that the method is not tractable for discontinuous functions. We prefer not

to use this name simply because it is not unique; simulated annealing methods using Monte Carlo, molecular dynamics, Brownian dynamics or other dynamics schemes could also be considered to be “continuous” minimizations. As discussed below, the method effectively samples the clusters’ energies from a Boltzmann distribution. Therefore, we suggest that the Press et al. method be called the “Boltzmann simplex”-simulated annealing (BSSA) algorithm. The BSSA algorithm is a modification of the downhill simplex (DS) algorithm, which is originally due to Nelder and Mead [11]. A brief review of the DS algorithm is therefore in order.

2.1. Description of the downhill simplex algorithm

The downhill simplex algorithm can be used to optimize a local minimum of an arbitrary function. The following description follows that of Press et al. [5]. Consider the optimization of a local minimum of the potential energy function $U(\mathbf{x})$, with \mathbf{x} the vector of Cartesian coordinates specifying the geometry of a cluster of N atoms. An initial set of $3N + 1$ initial cluster geometries in the vicinity of the local minimum must first be specified. Each geometry is referred to as a “vertex”. The set of $3N + 1$ vertices is called the “simplex”. The simplex defines a $(3N - 1)$ -dimensional polyhedron which encloses a $3N$ -dimensional hypervolume.

In the DS algorithm, the potential energy $U(\mathbf{x})$ is calculated at each of the $3N + 1$ vertices. At each point in the evolution of the simplex, a number of moves are possible. One is *reflection*. In a reflection move, the highest-energy vertex is reflected through the hyperplane formed by the other $3N$ vertices in such a way as to conserve the hypervolume of the simplex. This is generally the first move the algorithm tries.

After reflection, the DS algorithm carries out one of two other possible moves. A *reflection–expansion* may be attempted, which is a reflection move that increases the simplex’s hypervolume. This is done if the preceding reflection move gave a result lower in energy than the lowest point in the previous simplex, allowing the algorithm to move rapidly downhill where appropriate. If, however, the preceding reflection gave a result that was worse than the second-highest-energy vertex, a *contraction* is attempted. In a contraction, the highest vertex is moved along one

dimension away from its initial position towards the lowest-energy vertex.

If neither of the two preceding moves (contraction or reflection–expansion) improves the situation, the simplex carries out a *multiple contraction*. In a multiple contraction, the highest vertex is simultaneously moved along all the coordinates towards the lowest-energy vertex.

After the preceding series of move attempts has been made, in which the simplex may have moved as many as three times, the process is repeated until a convergence criterion is met or the maximum specified number of iterations is achieved. Press et al. [5] liken the evolution of a simplex to an amoeba which oozes along the potential energy surface.

The DS method will, within the usual limits of machine precision and effective termination criteria, converge to an accessible local energy minimum (unless multiple local minima are within “reach” of the initial simplex). However, in our experience with cluster systems we have found that the DS method is somewhat limited in its ability to completely resolve very shallow minima.

2.2. Description of the BSSA algorithm

The BSSA algorithm was developed as a general scheme for optimizing many-dimensional functions with multiple minima [5]. The BSSA algorithm proceeds in much the same way as the DS algorithm described above. The principal modification is the introduction of temperature-dependent random fluctuations into the energies of the simplex vertices at each step. This distinguishes the BSSA algorithm from a Monte Carlo walk, wherein geometries are subjected to random fluctuations which are either accepted or rejected according to a Boltzmann probability.

Thus, in the BSSA algorithm one generates an initial simplex. Then if \mathbf{x}^j represents a vertex, each vertex’s energy is subjected to random fluctuations of the form

$$U' = U(\mathbf{x}^j) + k_B T \ln(z) \quad (1)$$

where k_B is the Boltzmann constant in appropriate units and z is a random number on the interval (0,1). This method corresponds to “scrambling” the test vertices’ energies as if they were Boltzmann-distributed;

hence the name “Boltzmann simplex.” We use a variety of random number generators, including the `ran2` algorithm also presented by Press et al. [5], to generate z . In every other respect, the BSSA algorithm functions as a normal DS algorithm, with each new vertex’s energy subjected to a random fluctuation given by Eq. (1). Instead of wandering on the potential energy surface, the Brownian simplex wanders on a temperature-dependent pseudosurface. This pseudosurface becomes the actual potential energy surface in the limit $T \rightarrow 0$. By the same token, in this limit the BSSA algorithm becomes the DS algorithm. Also note that the usual caveats of the proper use of random number generators for long simulations apply here; even the best generator must be occasionally re-initialized to avoid periodic recurrence of the sequence [4,5].

The introduction of noise into the downhill simplex has the effect of making the BSSA algorithm into a “quasi-Metropolis” walk; as it cycles through its moves, the simplex will always move towards a lower-energy geometry if one is generated, but will also occasionally move uphill towards higher-energy geometries. This happens when the algorithm “mistakenly” takes a high-energy vertex to be a low-energy one. We have implemented the BSSA algorithm as presented by Press et al. in their `amebsa` routine [6] with some minor additions required by the application of the method to clusters. These additions are described in detail below.

2.3. Generating the initial simplex for cluster systems

The BSSA algorithm, like the DS algorithm, requires the user to supply an initial simplex. For a cluster composed of N atoms, a simplex of $3N + 1$ initial cluster geometries must therefore be specified. This can be done in a number of ways. We have chosen to use randomly generated initial configurations so as to avoid any bias that might be introduced into our calculations by a lucky (or unlucky) choice of initial conditions. In the studies of the argon clusters Ar_N , each atom was randomly placed within the interior of a cubic box. The size of the box was increased with the size of the cluster so as to keep the density approximately constant. Box sizes ranged roughly from 3 to 15 Å.

For simplex initiation of the water clusters $(\text{H}_2\text{O})_m$ (m is the number of water monomers in the cluster;

$N = 3m$), two boxes were specified. One large “cluster box” was used to generate random initial locations of the oxygen atom of each water molecule, while a second, smaller “molecular box” centered on each oxygen was used to randomly place the molecule’s hydrogen atoms in the vicinity of the oxygen atom. The cluster box ranged from 6 to 16 Å in size while the molecular box ranged from 3 to 4 Å. This method is only practical for potentials in which the individual water molecules in the cluster are allowed to be internally flexible. One could imagine trying more elaborate schemes for rigid-molecule interaction potentials, including random selection of the molecular center-of-mass within a cluster box followed by choosing a random orientation of a rigid, pre-optimized monomer about the center of mass [4]. Such a strategy might well be more efficient for studying flexible-molecule potentials as well, but we felt that random generation of initial conditions was a more stringent test of the algorithm’s effectiveness to initialize each molecule’s geometry well away from its minimum-energy structure. We also intended to avoid biasing our results by imposing restrictions on the molecules’ initial structures.

2.4. Annealing schedules

There is no unique formula for determining the rate at which the temperature should be reduced in simulated annealing work, or for determining how high the uppermost temperature should be. If the uppermost temperature T_h is sufficiently high, the BS walk is ergodic in configuration space as well as in the energy distribution, at least in the limit of infinite sampling. Thus an initial temperature for simulated annealing must be high enough to sample all relevant configurations of interest within a large but finite number of simplex iterations. We briefly discuss the selection of T_h in Section 3.1.

The temperature reduction must also be slow enough to allow the algorithm to “settle down” to the DS algorithm within the global minimum. However, the slower the temperature reduction, the longer the calculation will take. With this in mind, several annealing schedules were utilized and tested in order to get a better understanding of what would work best in practice, by using the prototypical Lennard–Jones Ar_N clusters as a test case.

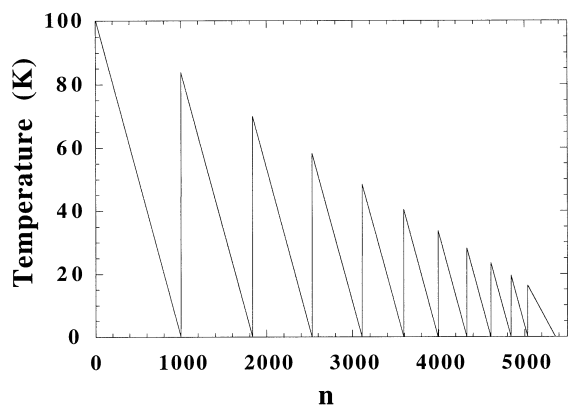


Fig. 1. Illustration of a typical “sawtooth” annealing schedule.

By trial and error, we found that some annealing schedules were more efficient than others. A simple linear annealing schedule of temperature reduction is sometimes employed in simulated annealing work, but we found that this schedule did not efficiently (i.e., with a minimum of computational effort) locate the known minimum-energy structures of these clusters. Similar problems were observed when the temperature was decreased exponentially, particularly as the clusters’ sizes increased. Of the schedules we tried, two worked the best at finding the minimum-energy structures within a reasonable number of sampled temperatures. For relatively small clusters, a very simple strategy was effective which we call the “sawtooth” schedule (see Fig. 1). The sawtooth schedule involved a linear decrease of the temperature

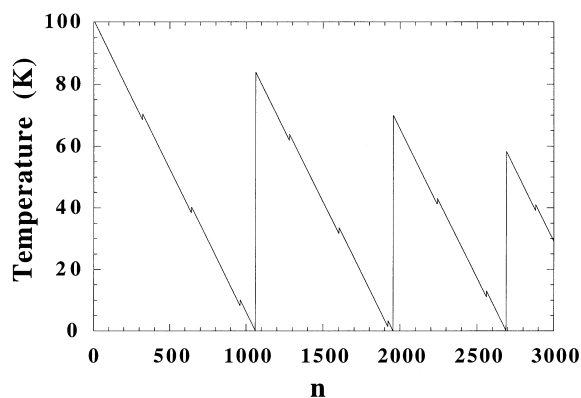


Fig. 2. Illustration of a typical “rasped sawtooth” annealing schedule.

from T_h to 0 K followed by a sequence of nine linear annealings from an upper temperature equal to 80–90% of the previous T_h down to 0 K again, with a final annealing from 10 K to 0 K at half the annealing rate of the previous 10 sawteeth. This schedule helps to ensure that if a cluster has several local minima available to it that are similar structurally but different in energy, the simplex had a good chance to find its way out of a local minimum if it became trapped in one by too rapid quenching.

For larger clusters, a slightly more complex annealing schedule was implemented. This sequence was similar to the simple schedule but contained multiple temperature fluctuations within a linear annealing. After every 150–300 steps of linear annealing, the final temperature was incremented by 20–40 times the decrement step. This resulted in a “jagged sawtooth” schedule (see Fig. 2). The jagged sawtooth schedule continues until the uppermost temperature for a sawtooth drops below 10 K, at which point the calculation is terminated. All calculations presented in this paper used this latter schedule.

2.5. Some additional details

Occasionally, one needs to restart a run which has either terminated prematurely due to system failure or which may not have been annealed slowly enough. One can, of course, periodically save the entire simplex, but as the size of the cluster becomes large storage can become an issue. Instead, we periodically save the lowest-energy vertex encountered thus far and, if necessary, we restart the algorithm using it as the starting point for the generation of a new initial simplex. Press et al. have recommended that a good choice for starting an ordinary simplex algorithm is obtained by picking a single geometry \mathbf{x}° and generating the i th vertex of the initial simplex by the formula

$$\mathbf{x}^i = \mathbf{x}^\circ + c * \mathbf{e} \quad (2)$$

where c is a small constant and \mathbf{e} is a $3N$ -dimensional unit vector [5]. In our restarts we generally set \mathbf{x}° equal to the lowest-energy structure found by the algorithm up to that point and use the formula above to generate $3N$ additional vertices. The parameter c is chosen appropriately to the system of

interest to generate structures that are close to the initial vertex.

Another consideration concerns the full resolution of the cluster geometries. As observed above, the BSSA algorithm becomes the DS algorithm when the temperature becomes exactly zero. The DS algorithm is, in our experience, extremely inefficient at converging shallow functions, especially shallow functions of many degrees of freedom. This observation seems to be independent of the precision with which the calculations are carried out and may be an intrinsic limitation of our implementation of Press et al.'s DS algorithm [5]. We therefore submitted the final output of each of our completely annealed BSSA calculations to minimization via Powell's quadratically convergent direction set method [12], presented by Press et al. as the `powell` routine [5]. This routine, which does not require the user to supply a routine for the calculation of the gradient, effectively resolves the local minimum of the cluster. We have not in any true sense combined the BSSA and Powell algorithms; however, such a combination is currently being investigated in our laboratory. Rather, this strategy follows the recommendations of a recent paper by Finnila et al. [13], in which gradient-based optimization was used as the final refinement step of a "quantum annealing" method.

Finally, the computational resources used in these calculations are worth mentioning. Most of our calculations were carried out on two Silicon Graphics workstations; an Iris Indigo R4000 (48 MB RAM) and an Iris Indy R4600 (96 MB RAM) under IRIX 5.3. Memory and storage requirements were so minimal that they were not assessed (less than 1 MB for each of the calculations reported here). CPU times on *unoptimized code* (i.e., interpolation methods to speed up the computation of cluster energies were not used [4], nor were special means employed to generate logarithmically-distributed random numbers [5]) ranged from a few minutes (small argon clusters) to 4.5 days (hexamer water clusters). These times are anecdotally similar to times required for Monte Carlo simulations. Fundamentally, the CPU time per cycle of these calculations is limited by the speed with which the potential energy of each vertex is computed. More study is needed to fully assess the efficiency of the BSSA algorithm relative to other available methods.

3. Results and discussion

3.1. Argon clusters

We first consider argon clusters within the approximation of the well-known Lennard–Jones pair potential, for benchmarking the BSSA algorithm against the results of Hoare and Pal [6,7]. This potential is given by Eq. (3) below:

$$U = 4\epsilon \sum_{i=1}^{N-1} \sum_{j=i+1}^N \left[\left(\frac{\sigma}{r_{ij}} \right)^{12} - \left(\frac{\sigma}{r_{ij}} \right)^6 \right] \quad (3)$$

Here ϵ is the dimer well depth and σ is the dimer core radius. If this model is used to model argon, appropriate parameter values for this system are $\epsilon = 121$ K (0.0003832 atomic units) and $\sigma = 3.4$ Å [14]. It is conventional to set ϵ and σ equal to 1 when tabulating data and carrying out calculations, as these parameters can be appropriately rescaled at the end of the day (see [13]).

For the Lennard–Jones cluster calculations, the upper temperatures were chosen by two methods: (1) trial and error, and (2) computing the root-mean-square (r.m.s.) fluctuations of randomly selected cluster energies and scaling the result by the Boltzmann constant to obtain a temperature. This latter method was suggested to us by one of the ECC3 conference attendees, who used an analogous method in a different context [15]. We initially carried out annealing runs using the first approach, but since the conference we have repeated our calculations by using the r.m.s. temperatures and here present them instead. The calculations presented here were also annealed much more slowly than those presented in the conference. The annealing decrement ranged from about 2×10^{-4} K to 2×10^{-2} K, depending on the size of the cluster in question. Annealed geometries were subsequently refined by the Powell method [5]. The results, and comparison with literature values [6], are shown in Table 1.

The energies of clusters with $N < 9$ are seen to be in excellent agreement with the values obtained from the literature; visual inspection of the cluster geometries confirmed that the proper symmetries were obtained. However, for larger N the minimum-energy structures were not successfully located. We observed that slower and slower annealing rates continued to improve our results. Presumably, even slower

Table 1
Uppermost annealing temperatures (K) and energies (relative to ϵ) of Lennard–Jones clusters

N	T_h^a	Cluster energy		
		Present work	[6]	% Difference
2	25.9	–1.000	–1.000	0.0
3	44.9	–3.000	–3.000	0.0
4	63.5	–6.000	–6.000	0.0
5	81.0	–9.104	–9.103	0.0
6	99.8	–12.71	–12.71	0.0
7	119	–16.51	–16.51	0.0
8	140	–19.82	–19.82	0.0
9	165	–23.17	–24.11	3.9
10	192	–27.56	–28.42	3.0
11	224	–30.94	–32.77	5.6
12	260	–37.15	–37.97	4.8
13	301	–41.44	–44.33	6.5

^a T_h obtained from root-mean-square energy fluctuations of a uniform random sample of cluster geometries, as suggested in [15].

annealing rates will successfully converge the larger clusters. The energy surface for Lennard–Jones clusters has many minima that are close in energy to one another (for $N = 13$ there are 988 known minima [16]) and to the global minimum, owing to the extreme shallowness of the atom–atom potential. In this situation it is hard for the BSSA algorithm to find the global minimum unless a glacially slow annealing schedule is used.

3.2. Water clusters

The potential energy surface for the water clusters was represented by a model recently developed by Ferguson for bulk liquid water simulations [8]. The potential energy function was developed by adding intramolecular flexibility to the rigid SPC model [9]. The cluster energy is given by

$$U = k_l \sum_{\text{bonds}} [(l - l^\circ)^2 + k_{cub}(l - l^\circ)^3] + k_\theta \sum_{\text{angles}} (\theta - \theta^\circ)^2 + \sum_{\text{O-O}} \left(\frac{A}{r_{ij}^{12}} - \frac{B}{r_{ij}^6} \right) + \sum_{\text{charges}} \frac{q_i q_j}{r_{ij}} \quad (4)$$

The parameters for this potential are summarized in Table 2. In the annealing calculations, T_h ranged from 100 to 300 K, and was chosen through trial and error. The temperature decrement was chosen so as to allow 8000 to 10 000 temperatures within the annealing run, with a maximum of 10 000 BSSA iterations per

temperature. We were able to reproducibly obtain all cluster geometries given here using a range of annealing parameters and schedules, and believe that these are the lowest-energy structures that this model admits. However, it is impossible to prove that this is the case for finite sampling rate and iteration number.

We first considered the $(\text{H}_2\text{O})_2$ cluster. The geometric parameters of the minimum-energy structure, and comparisons with published Hartree–Fock (HF) values [17], are given in Table 3. The values obtained from the Ferguson potential [8] are qualitatively similar to the HF results, but are not in quantitative agreement. The Ferguson model predicts a smaller O–O distance and larger intramolecular O–H distances; however, note that in all cases the length of the hydrogen-bonded O–H bond is greater than all

Table 2
Parameters of the $(\text{H}_2\text{O})_m$ interaction potential from [8]

Parameter	Value	Units
k_l	547.5	kcal mol ⁻¹ Å ⁻²
l°	1.0	Å
k_{cub}	–1.65	Å ⁻¹
k_θ	49.9	kcal mol ⁻¹ rad ⁻¹
θ	109.5	deg
A	650 000	kcal mol ⁻¹ Å ¹²
B	625.47	kcal mol ⁻¹ Å ⁶
q_H	+0.413	kcal ^{1/2} Å ^{1/2} mol ^{-1/2}
q_O	–0.826	kcal ^{1/2} Å ^{1/2} mol ^{-1/2}

Table 3
Comparison of predicted (H₂O)₂ structure parameters with literature values

Method	r_{1a}^a	r_{1b}	θ_1^a	R^a	r_{2a}	θ_2	r_{2b}
HF/4-31G ^b	0.949	0.958	111.3	2.832	0.951	112.0	—
HF/6-31G ^{*b}	0.947	0.952	105.4	2.971	0.948	105.9	—
HF/6-31G ^{**b}	0.942	0.948	106.2	3.031	0.944	106.2	—
Present work	0.999	1.019	107.7	2.748	1.006	108.4	1.003

^a The r_{jk} are the internal bond lengths of the j th molecule (Å), with r_{1b} the length of the hydrogen-bridging O–H bond; R is the oxygen–oxygen distance (Å). θ_j is the internal angle of the j th water molecule (deg).

^b Hartree–Fock calculations from [17]. A dash (—) means that the information was not available from the cited source.

other O–H bonds, which seems chemically reasonable. In Table 4, we present our results for the (H₂O)₃ cluster. The cluster geometry is shown in Fig. 3. The oxygen atoms are arranged in an equilateral triangle, with the hydrogen of each molecule pointing towards the oxygen of the next molecule. We again note that the values for the internal bonds calculated with the Ferguson model are a little higher than those predicted by Hartree–Fock calculations [17]. However, the internal angles are in reasonably good agreement with the ab initio results. All the predicted trimer configurations are cyclic triangular structures, in agreement with vibration–rotation tunneling (VRT) spectroscopy [10,18] and density-functional theory calculations [19].

In Table 5 we list the geometric parameters predicted by the Ferguson model for (H₂O)₄. The

Table 4
Comparison of predicted (H₂O)₃ structure parameters with literature values

Parameter	HF/6-31G ^{*b}	Present work
r_{1a}^a	0.956	1.027
r_{1b}	0.947	1.005
r_{2a}	0.956	1.020
r_{2b}	0.947	1.000
r_{3a}	0.956	1.021
r_{3b}	0.948	1.001
R_{12}^a	2.876	2.736
R_{13}	2.864	2.754
R_{23}	2.864	2.756
θ_1^a	106.2	107.8
θ_2	106.0	107.1
θ_3	105.8	107.2

^a The r_{jk} are the internal bond lengths for the j th molecule (Å), the R_{jp} are the oxygen–oxygen distances between molecules j and p (Å), and θ_j is the internal angle for the j th water molecule (deg).

^b Hartree–Fock calculation. See [17].

minimum-energy structure is displayed in Fig. 4. The structure is a ring-like arrangement of the molecules' oxygen atoms, with one oxygen puckered by 17° above the plane formed by the other three. Again, this result is qualitatively similar to geometries obtained from both theory and experiment [10,17,19,20].

The results of the calculations of the pentamer and hexamer water clusters are presented in Tables 6 and 7, respectively. The structures of the pentamer and hexamer may be viewed in Figs. 5 and 6, respectively. The calculated structure of the pentamer is a cyclic, puckered ring with one oxygen raised up above the plane formed by the other four oxygens. This is in qualitative agreement with recent VRT experiments and calculations by Liu, Saykally and co-workers [10], which indicate that the distance between oxygen atoms is between 2.759 and 2.84 Å and that the pentamer is a puckered ring. Calculated values for this distance according to Hartree–Fock (HF), Møller–Plesset second-order perturbation (MP2) and density-functional theory (DFT) ranged from 2.73 Å (DFT) to 2.9 Å (HF) [10,19]. The values obtained from the

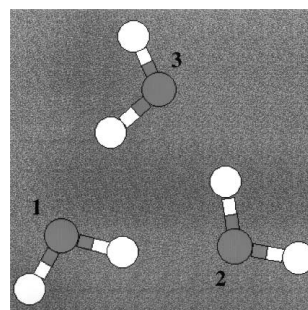


Fig. 3. Minimum-energy structure of (H₂O)₃ predicted by the Ferguson model.

Table 5
Predicted (H₂O)₄ structure parameters

Parameter	Value	Parameter	Value	Parameter	Value
r_{1a}^a	1.029	R_{12}^a	2.705	θ_1^a	106.9
r_{1b}	1.002	R_{13}	3.814	θ_2	106.2
r_{2a}	0.999	R_{14}	2.708	θ_3	106.1
r_{2b}	1.027	R_{23}	2.694	θ_4	106.6
r_{3a}	1.001	R_{24}	3.777		
r_{3b}	1.027	R_{34}	2.708		
r_{4a}	1.003				
r_{4b}	1.029				

^a The r_{jk} are the internal bond lengths for the j th molecule (Å), the R_{jp} are the oxygen–oxygen distances between molecules j and p (Å), and θ_j is the internal angle for the j th water molecule (deg).

Ferguson potential for the pentamer are thus well within the range of the ab initio calculations and experimental results.

The hexamer cluster is a most interesting case, with different theoretical methods and models yielding very different structures. Density-functional theory calculations predict that the hexamer is a distorted, cage-like structure with seven hydrogen bonds [19]. Comparison of recent VRT spectroscopy results with diffusion Monte Carlo calculations have led to the suggestion that the minimum-energy structure has a cage-like configuration held together by eight hydrogen bonds [10]. The SPC/E and POL1 models predict a bicyclic ring structure with seven hydrogen bonds [21]. Within the Ferguson potential, we find a structure which is somewhat ring-like but has one molecule's oxygen atom above the plane of a ring formed

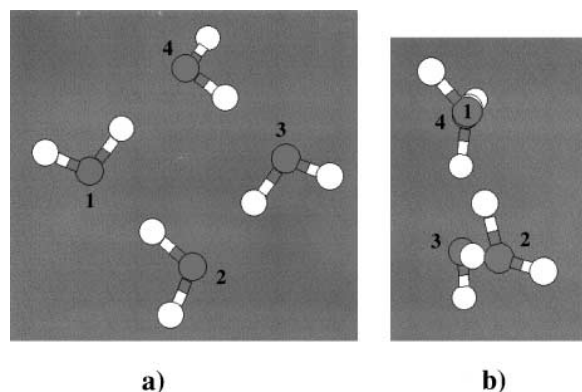


Fig. 4. Minimum-energy structure of (H₂O)₄ predicted by the Ferguson model. (a) Top view; (b) edge-on view.

Table 6
Predicted (H₂O)₅ structure parameters

Parameter	Value	Parameter	Value	Parameter	Value
r_{1a}^a	1.029	R_{12}^a	2.687	θ_1^a	107.4
r_{1b}	1.002	R_{13}	4.191	θ_2	106.2
r_{2a}	1.029	R_{14}	4.496	θ_3	105.1
r_{2b}	1.001	R_{15}	2.734	θ_4	107.2
r_{3a}	1.023	R_{23}	2.710	θ_5	104.9
r_{3b}	1.000	R_{24}	4.151		
r_{4a}	1.032	R_{25}	4.131		
r_{4b}	1.003	R_{34}	2.702		
r_{5a}	1.001	R_{35}	3.975		
r_{5b}	1.026	R_{45}	2.717		

^a The r_{jk} are the internal bond lengths for the j th molecule (Å), the R_{jp} are the oxygen–oxygen distances between molecules j and p (Å), and θ_j is the internal angle for the j th water molecule (deg).

by four oxygens, with a second below the plane. This structure has only six hydrogen bonds.

It would be interesting to use the Ferguson potential model as input for diffusion Monte Carlo calculations to see whether reasonable agreement with experiment might be obtained from this apparently new hexamer structure. It is possible that there is a competition between ring-like and cage-like forms in the hexamer, and that different models will tend to variously favor one or the other. Similar phenomena have been observed in simulations of other cluster systems [3,22]. Thermodynamic computations of the hexamer cluster may shed some light on this by using Monte

Table 7
Predicted (H₂O)₆ structure parameters

Parameter	Value	Parameter	Value	Parameter	Value
r_{1a}^a	1.029	R_{12}^a	2.684	R_{45}	2.717
r_{1b}	1.003	R_{13}	4.618	R_{46}	4.503
r_{2a}	1.027	R_{14}	5.108	R_{56}	2.701
r_{2b}	0.999	R_{15}	4.664		
r_{3a}	1.029	R_{16}	2.704	θ_1^a	106.7
r_{3b}	1.000	R_{23}	2.695	θ_2	104.4
r_{4a}	1.000	R_{24}	4.330	θ_3	105.7
r_{4b}	1.024	R_{25}	5.330	θ_4	103.7
r_{5a}	1.028	R_{26}	4.644	θ_5	106.2
r_{5b}	1.001	R_{34}	2.708	θ_6	105.0
r_{6a}	1.029	R_{35}	4.585		
r_{6b}	1.001	R_{36}	5.320		

^a The r_{jk} are the internal bond lengths for the j th molecule (Å), the R_{jp} are the oxygen–oxygen distances between molecules j and p (Å), and θ_j is the internal angle for the j th water molecule (deg).

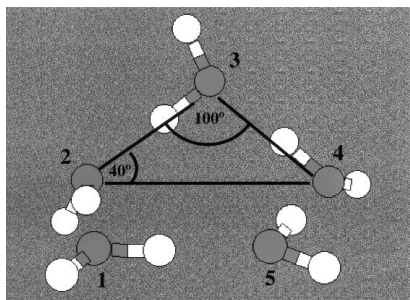


Fig. 5. Minimum-energy structure of $(\text{H}_2\text{O})_5$ predicted by the Ferguson model.

Carlo jump-walking techniques to ensure proper sampling of any and all coexisting isomers [3,23–25].

4. Conclusions

Global optimization algorithms which do not require explicit computation of the gradient are attractive for a variety of applications. The BSSA algorithm by Press et al. [5] is one such algorithm. BSSA was able to approximately locate the minimum-energy structures for many of the argon clusters considered; however, the results usually had to be passed to a

Powell steepest-descent algorithm to converge the clusters' energies completely. This combination of techniques was found to be reasonably effective. Even so, the BSSA algorithm occasionally (i.e., for large clusters) became lodged in a local minimum, a problem which was dealt with by using extremely slow annealing rates. It is likely that the BSSA algorithm itself is simply not well-tuned to deal with the extremely shallow, multivalued potential energy surface exhibited by Lennard–Jones clusters and may need to be modified somewhat for this kind of application. We are planning a series of modifications, including the possibility of quenching minima located at higher temperatures in the schedule occasionally with the Powell method. We also are exploring other global optimization schemes, such as genetic algorithms [26,27].

In our study of small water clusters, we compared minimum-energy cluster structures predicted by the Ferguson model [8], which is known to successfully describe many properties of bulk liquid water, with experimental and theoretical results. It is extremely important to point out that unless one includes zero-point motions and tunneling in such a calculation, one may or may not get quantitative agreement with experiment if these effects can affect which geometry is favored free-energetically. This caveat is especially important for small water clusters, and diffusion Monte Carlo calculations have proved to be valuable [9,16,21,22]. If the clusters are “warm”, then thermal effects probably need to be included as well, suggesting a quantum-path-integral approach [3].

Overall we found that the Ferguson model yielded excellent qualitative agreement with experiment and high level ab initio calculations for clusters with up to five water molecules. Notably, the Ferguson model correctly predicts that the $(\text{H}_2\text{O})_5$ pentamer cluster is a puckered ring. However, for the hexamer cluster, the model predicts that a ring structure is the lowest-energy geometry. Comparisons of recent experimental work with diffusion Monte Carlo studies with other potential models as input [28,29] have given some evidence that the structure may be cage-like. Comparison of diffusion Monte Carlo calculations using the Ferguson model with experiment might shed some light. It would also be interesting to carry out global minimization studies on still larger clusters within this potential than have yet been

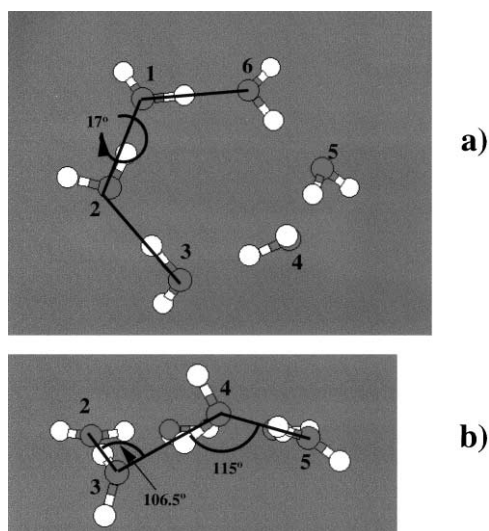


Fig. 6. Minimum-energy structure of $(\text{H}_2\text{O})_6$ predicted by the Ferguson model. (a) Top view; (b) Edge-on view.

characterized experimentally [19,21]. Such calculations are in progress.

Our hope is that studies of the present type, wherein we evaluate potentials in terms of how well they can represent both bulk phase and cluster properties, can provide useful clues for reaching the “Holy Grail” — a potential energy model for water that accurately describes the properties of water in its solid, liquid, vapor and cluster phases.

Acknowledgements

F.T. and R.Q.T. would like to thank David Ferguson for sharing preprints of his work and letting us have a copy of his Fortran code for computing the energy of bulk liquid water, which helped us debug our own implementation for cluster work. R.Q.T. has also benefited from helpful conversations with David Freeman, M. Ramakrishnan and (during this conference) Stephen Gray regarding simulated annealing techniques. We gratefully acknowledge the Cooper Union Research Foundation and the Cooper Union School of Engineering for providing support for this research. The molecular structure figures were created with the help of the Xmol visualization tool [30]. Helpful comments from the referee resulted in an improved manuscript.

References

- [1] G. Benedek, T.P. Martin, G. Pacchioni (Eds.), *Elemental and Molecular Clusters*, Springer-Verlag, New York, 1988.
- [2] J.P.K. Doye, D.J. Wales, *Science* 271 (1996) 484.
- [3] D.L. Freeman, J.D. Doll, *Annu. Rev. Phys. Chem.* 47 (1996) 43.
- [4] M.P. Allen, D.F. Tildesley, *Computer Simulation of Liquids* (corrected 2nd printing), Oxford Science, Ipswich, UK, 1989.
- [5] W.H. Press, S.A. Teukolsky, W.T. Vetterling, B.P. Flannery, *Numerical Recipes in FORTRAN: The Art of Scientific Computing*, 2nd edn, Cambridge University Press, Cambridge, 1992.
- [6] M.R. Hoare, P. Pal, *Adv. Phys.* 20 (1971) 161.
- [7] M.R. Hoare, *Adv. Chem. Phys.* 40 (1979) 48.
- [8] D. Ferguson, *J. Comput. Chem.* 16 (1995) 501.
- [9] H.J.C. Berendsen, J.P.M. Postma, W.F. Van Gunsteren, J. Hermans, in: B. Pullman (Ed.), *Intermolecular Forces*, Reidel, Dordrecht, 1981.
- [10] K. Liu, J.D. Cruzan, R.J. Saykally, *Science*, 271 (1996) 929; K. Liu, M.G. Brown, C. Carter, R.J. Saykally, J.K. Gregory, D.C. Clary, *Nature*, 381 (1996) 501; K. Liu, M.G. Brown, J.D. Cruzan, R.J. Saykally, *Science*, 271 (1996) 62.
- [11] J.A. Nelder, R. Mead, *Computer Journal* 7 (1965) 308.
- [12] R.P. Brent, *Algorithms for Minimization Without Derivatives*, Prentice-Hall, Englewood Cliffs, NJ, 1973.
- [13] A.B. Finnila, M.A. Gomez, C. Sebenik, C. Stenson, J.D. Doll, *Chem. Phys. Lett.* 219 (1994) 343.
- [14] E. Blaisten-Barojas, in: G. Benedek, T.P. Martin and G. Pacchioni (Eds.), *Elemental and Molecular Clusters*, Springer-Verlag, New York, 1988.
- [15] S.K. Gray, D.E. Manolopoulos, *J. Chem. Phys.* 104 (1996) 7099.
- [16] F.H. Stillinger, D. Stillinger, *J. Chem. Phys.* 93 (1990) 6013.
- [17] E. Honegger, S. Leutmyler, *J. Chem. Phys.* 88 (1988) 2582.
- [18] N. Pugliano, R.J. Saykally, *Science* 257 (1992) 1937.
- [19] C. Lee, H. Chan, G. Fitzgerald, *J. Chem. Phys.* 102 (1995) 1266.
- [20] J.D. Cruzan, L.B. Braly, K. Liu, M.G. Brown, J.G. Loeser, R.J. Saykally, *Science* 271 (1996) 59.
- [21] L.S. Sremaniak, L. Perera, M.L. Berkowitz, *J. Chem. Phys.* 105 (1996) 3715.
- [22] G.E. Lopez, D.L. Freeman, *J. Chem. Phys.* 98 (1993) 1428.
- [23] D.D. Frantz, D.L. Freeman, J.D. Doll, *J. Chem. Phys.* 93 (1990) 2769.
- [24] D.D. Frantz, D.L. Freeman, J.D. Doll, *J. Chem. Phys.* 97 (1992) 5713.
- [25] A. Matro, D.L. Freeman, R.Q. Topper, *J. Chem. Phys.* 104 (1996) 8690.
- [26] S.K. Gregurick, M.H. Alexander, B. Hartke, *J. Chem. Phys.* 104 (1996) 2684.
- [27] R. Judson, in: K.B. Lipkowitz, D.B. Boyd (Eds.), *Reviews in Computational Chemistry*, Vol. 10, VCH Publishers, New York, 1997, pp. 1–73.
- [28] D.J. Wales, T.R. Walsh, *J. Chem. Phys.* 105 (1996) 6957.
- [29] D.J. Wales, *Science* 271 (1996) 925.
- [30] Xmol, version 1.3.1, Minnesota Supercomputer Center, Inc., Minneapolis MN, 1993.